Insights from the first winter weather observations near Mount Everest's summit

Tenzing Chogyal Sherpa[1], Tom Matthews[2], L. Baker Perry[3], Amrit Thapa[1,4], Praveen Kumar Singh[5], Arbindra Khadka[1,6], Inka Koch[7], Mauri Pelto[8], Prajjwal Panday[8], Deepak Aryal[9], Dibas Shrestha[9], Shichang Kang[10] and Paul Andrew Mayewski[11]

[1]*International Centre for Integrated Mountain Development, Kathmandu, Nepal*
[2]*Department of Geography, King's College London, UK*
[3]*Appalachian State University, Boone, North Carolina, USA*
[4]*Geophysical Institute, University of Alaska Fairbanks, Fairbanks, Alaska, USA*
[5]*Indian Institute of Technology Roorkee, Uttarakhand, India*
[6]*University of Grenoble Alpes, CNRS, IRD, IGE, Grenoble, France*
[7]*Department of Geosciences, University of Tübingen, Germany*
[8]*Department of Environmental Science, Nichols College, Dudley, Massachusetts, USA*
[9]*Central Department of Hydrology and Meteorology, Tribhuvan University, Kirtipur, Nepal*
[10]*State Key Laboratory of Cryospheric Science, Northwest Institute of Eco-Environment and Resources, Chinese Academy of Sciences, Lanzhou, China*
[11]*Climate Change Institute, University of Maine, Orono, Maine, USA*

Reaching up to 8849m above mean sea level (asl), the upper slopes of Mount Everest provide one of the most climatically extreme environments on the planet. It is also an environment likely to be warming rapidly, due to the tendency for temperature increases to amplify at greater elevations in the troposphere under climate change (Pepin *et al*., 2015). However, our understanding of high-altitude climates has been severely limited by an understandable lack of basic *in situ* observations (Matthews, 2020a). The logistical demands associated with climbing to such heights challenges the initial installation of automatic weather stations (AWSs). Those AWSs which do get deployed must then withstand extreme cold and severe winds if they are to remain operational. Mountain regions that are hardest to reach, at those times of year when the weather is most extreme, have therefore been monitored least, meaning winter conditions on the planet's highest peaks remain largely a mystery. Through necessity, insights have mostly been taken from relatively coarse reanalysis data (Moore and Semple, 2011; Matthews *et al*., 2021).

Not only does this monitoring gap represent a technical blind spot in the understanding of our planet's climate envelope, but the practical impacts for society may also be substantial. For example, the mountains of the Hindu Kush Himalayan region store the largest mass of ice outside the poles (Bolch *et al*., 2012), and the ongoing retreat is a major concern for regional freshwater security (Immerzeel *et al*., 2020; Nie *et al*., 2021). The potential future losses inferred by modelling studies is, therefore, of much relevance for resource management and hazard planning (Huss and Hock, 2018). However, such outlooks are underpinned by an understanding of glacier–climate interactions that is biased towards more accessible regions and seasons in the same way the observations are. Temperature index models, for example, are widely used for glacier mass balance projections (Hock *et al*., 2019), but they appear unsuited to capture the important role of sublimation, which is amplified at higher altitudes (Stigter *et al*., 2018; Litt *et al*., 2019) and in the winter season (Wagnon *et al*., 2013).

In this short article, we address the issues raised above by assessing the first observations from winter recorded by the one of the world's highest weather station networks on Mount Everest. We include the most-constrained estimate yet of air temperatures and cold stress on the summit, and we consider mechanisms of mass loss from the highest glacier on Earth.

Data and methods

We use meteorological data from the weather station network installed by the 2019 National Geographic and Rolex Everest Expedition, which is described by Matthews *et al*. (2020a,b) and summarised in Table 1. We summarise the weather across the full (>4500m) elevational range using simple descriptive statistics. For the summit – which sits ~400m above the Balcony AWS – we estimate air temperatures and cold stress using the temperature lapse rate and the assumption that wind speeds are the same as at the South Col AWS (which is situated in a less sheltered location than the Balcony). The temperature lapse rates were calculated as a linear regression of hourly temperature at the AWSs against elevation (cf. Immerzeel *et al*., 2014; Heynen *et al*., 2016), after first smoothing all temperatures with a running 24-hour mean to reduce the impact of solar heating which may affect measurements during brief spells of light winds (Matthews *et al*., 2020a,b).

Wind chill temperature (WCT) and facial frostbite time (FFT) were then computed with the estimated summit air temperature and wind speed following Moore and Semple (2011):

$$\mathrm{WCT} = 13.12 + 0.621\,T - 11.37\,V^{0.16} + 0.3965\,T\,V^{0.16} \quad (1)$$

$$\mathrm{FFT} = (-24.5\,(0.667V + 4.8) + 2111)(-4.8 - T)^{-1.688} \quad (2)$$

in which T is the air temperature (°C) and V is the wind speed (kmh^{-1}). Strictly, the latter refers to a reference height of 10m above the surface, whereas the Everest weather stations' wind sensors are at approximately two metres above ground, a height at which wind speeds are likely slower due to friction with the land surface. Hence, this should lead to a high (warm) bias in WCT. However, the equation is also strictly valid for an air density between two and three times higher

The views and interpretations in this publication are those of the author's and are not necessarily attributable to their organisations.

Table 1

Specifications of all the automatic weather stations installed across the slopes of Mount Everest.

	Phortse	*Base Camp*	*Camp II*	*South Col*	*Balcony*
Latitude (°N)	27.8456	27.9952	27.9810	27.9719	27.9826
Longitude (°E)	86.7472	86.8406	86.9023	86.9295	86.9292
Elevation (m asl)	3810	5315	6464	7945	8430
Operation	24 April 2019 to present	10 October 2019 to present	9 June 2019 to present	22 May 2019–18 July 2021	23 May 2019–1 January 2020

Abbreviation: m asl, metres above mean sea level.

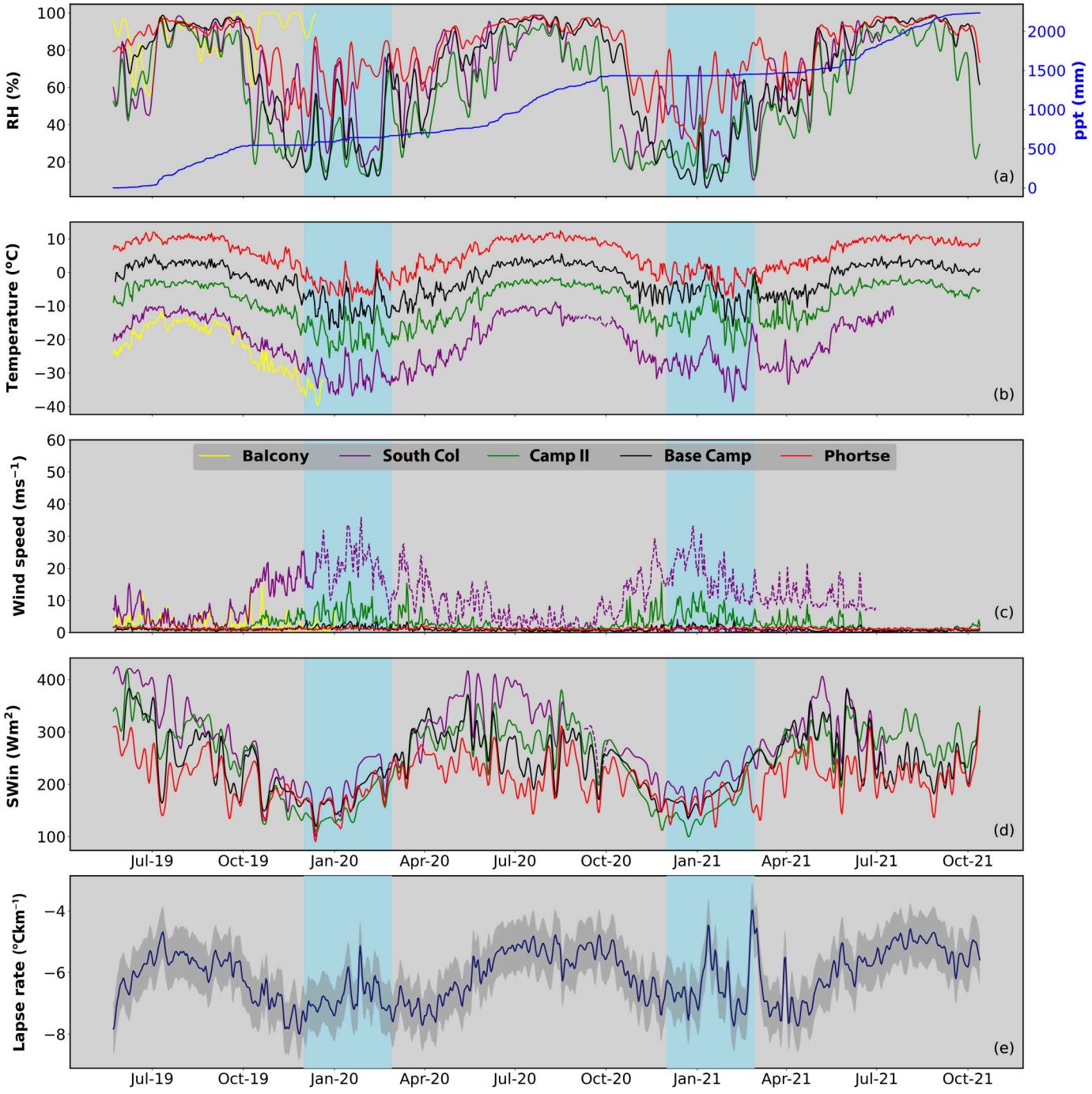


Figure 1. Mean daily values of selected variables from the automatic weather stations (AWSs). (a) Relative humidity; blue line in the panel represents cumulative precipitation at Phortse, (b) daily temperature, (c) average wind speed, (d) incoming solar radiation and (e) lapse rates across all stations. The lapse rates were calculated as the slope coefficient from regressing running 24-h mean air temperature at the AWSs against their elevations. The dashed line in all the plots represents data filled from ERA5 reanalysis data at South Col. For all the panels, the blue shaded region represents the winter season (DJF).

Table 2

Seasonal daily mean values estimated at the summit. The standard deviation values are represented by the plus/minus terms.

Season	*T (°C)*	*WS (ms⁻¹)*	*WCT (°C)*	*FFT (min)*
Monsoon (JJAS)	−18.8 ±2.7	5.2 ±2.6	−28.1 ±4.8	9.8 ±3.6
Post-monsoon (ON)	−30.1 ±4.7	13.9 ±6.7	−48.4 ±9.1	2.7 ±2.1
Spring (MAM)	−32.1 ±5.7	9.6 ±4.7	−48.5 ±8.8	3 ±1.6
Winter (DJF)	−37.3 ±4.4	18 ±6.5	−61.2 ±8.5	1.3 ±0.8

Abbreviations: FFT, facial frostbite time; WCT, wind chill temperature; WS, wind speed
JJAS: June, July, August, September; WS: Wind speed; MAM: March, April, May; DJF: December, January, February; ON: October, November

than at the summit of Everest, translating to a low (cold) bias in our application. Following Moore and Semple (2011), we assume that these biases approximately cancel.

To explore point surface mass balance during the winter of the world's highest glacier (South Col Glacier, hereafter the SCG), we use data from the South Col AWS (7945m asl). This station was the highest of the network installed in 2019 that was equipped with all the sensors required to resolve the surface energy balance (SEB) and is separated from the SCG by a horizontal distance of only a few hundred metres. We use COSIPY (the COupled Snowpack and Ice surface energy and mass balance model in PYthon: Sauter & Schneider, 2015) to infer the SEB for the SCG, with mass input via snowfall estimated from the precipitation recorded at Phortse (3810m asl). We set all COSIPY model parameters (e.g. roughness lengths) as in Potocki *et al.* (2022). We fill brief periods of missing data at the South Col with ERA5 reanalysis data (Hersbach *et al.*, 2020) downscaled to the AWS using machine learning (see Potocki *et al.*, 2022 for details). The initial snow depth (0.94m) for the COSIPY simulation model was taken from the 1km² Sentinel-1 snow depth product for 13 May 2019 (Lievens *et al.*, 2019), which is 10 days prior to the installation of the AWS (and the beginning of the COSIPY model run). Given the highly variable topography, the accuracy of this Sentinel product for the SCG is questionable; however, it is the highest resolution snow depth product, and preliminary analysis (not shown) indicated low sensitivity to initial snow depth in the COSIPY simulations.

Results

Winter stands distinct from the other seasons, with air temperatures and insolation plunging to their lowest values and wind speeds reaching their peak (Figure 1). The highest (3s) gust recorded by the network (66ms⁻¹; not shown) was indeed recorded at the South Col during January 2020 – immediately before the wind sensors went offline. The change to colder, conditions at the onset of winter generally magnifies with elevation, as the lapse rate steepens in this season meaning air temperatures fall more rapidly with height (Figures 1a and e). Relative humidity is noteworthy in winter because of its very high variability at synoptic timescales (Figure 1a). Although not quite as pronounced, the same high-frequency variance is evident in the air temperatures (Figure 1b). We attribute this wintertime peak in transitions between warmer, moister air masses and cooler, drier circulations, to the arrival of the Subtropical Jet over the Himalaya. The passage of waves in this westerly flow drives the variation in air mass character; and wind speeds peak when the jet axis crosses Everest (Matthews *et al.*, 2020b).

The elevation-enhanced drop in air temperature with the arrival of winter, combined with the amplification of winds, compound to generate extreme conditions of profound cold stress for the summit. The mean winter WCT is −61.2°C (Table 2), whilst the lowest daily mean observed during the period of observation was −77°C (on 31 December 2020) (Figure 2). The individual hour with the lowest WCT on the other hand reached −83°C, when the mean wind speed was 36ms⁻¹ and the temperature

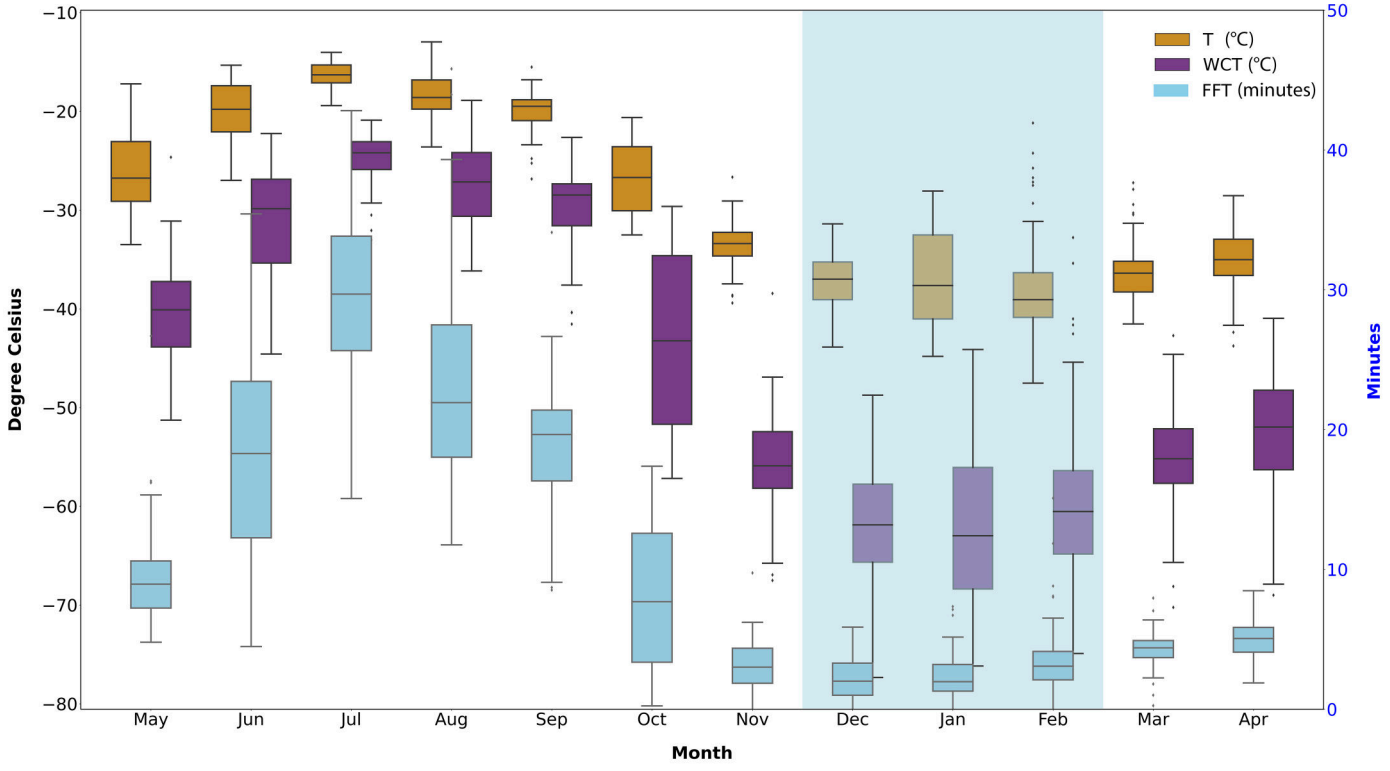


Figure 2. Boxplot of daily mean air temperature, wind chill temperatures (WCTs) and facial frostbite time (FFT) estimated at the summit. The FFT is plotted on the right y-axis. The horizontal line within the box denotes the median, whereas the first and third quartile are represented by the top and bottom of the box, respectively. The whiskers indicate the range (minimum and maximum values), and the points indicate values that are greater than 1.5 times the upper quartile and are often regarded as outliers. The blue shaded region represents winter season.

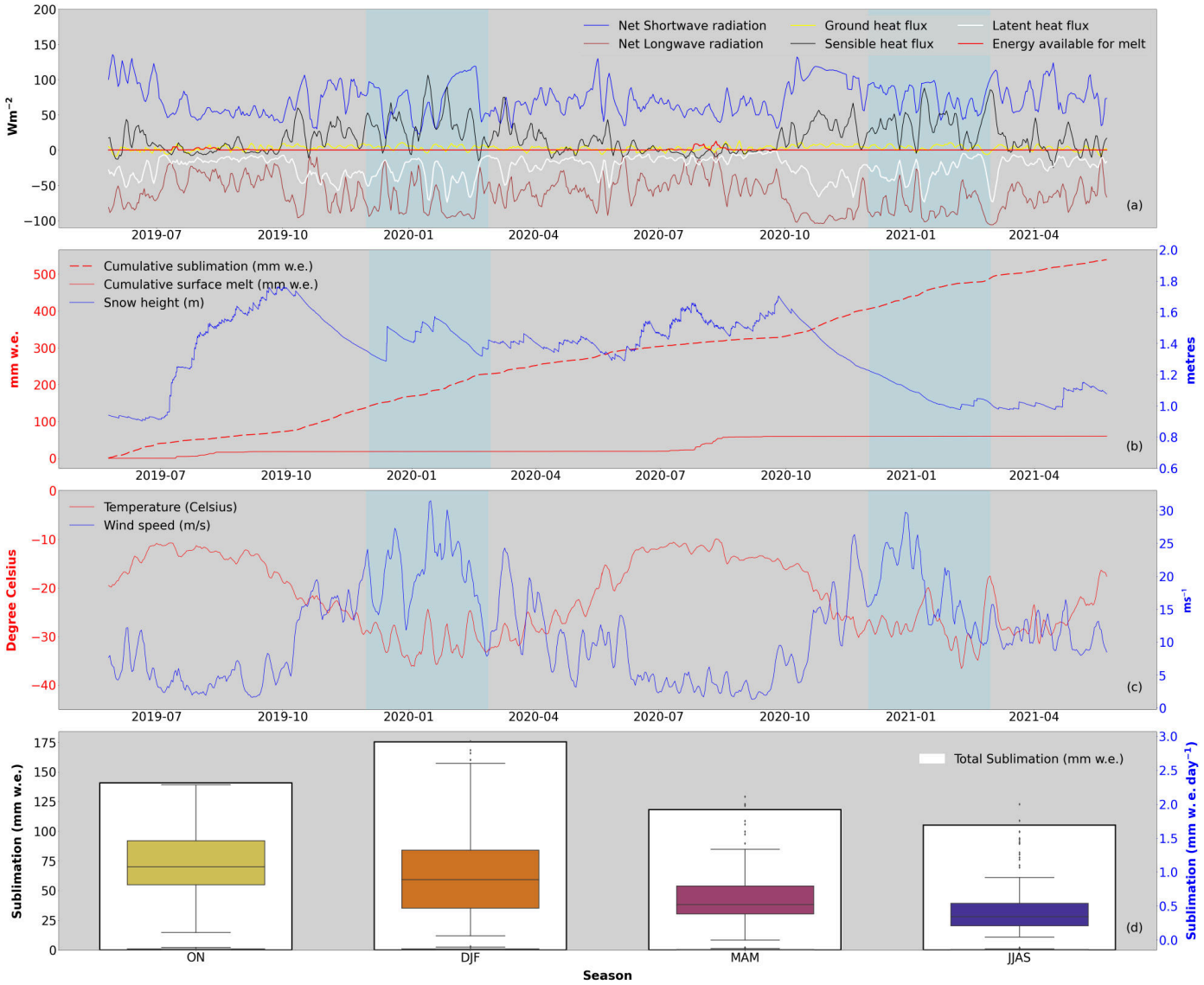


Figure 3. (a) Mean daily energy fluxes at South Col. (b) Cumulative surface melt and sublimation. The secondary axis represents the snow depth over the simulation period. (c) Temperature and wind speed (secondary axis) at South Col. (d) Bar plot of total sublimation in each season and boxplot of seasonal variation of daily sublimation rates in each season. The bar plot is plotted on the left y-axis, whereas the box plots are plotted against the right y-axis. The horizontal line within the box denotes the median, whereas the first and third quartile are represented by the top and bottom of the box, respectively. The whiskers indicate the range (minimum and maximum values), and the points indicate values that are greater than 1.5 times the upper quartile and are often regarded as outliers. From panels (a)–(c), the blue shaded region represents the winter season (DJF).

was −48°C (in 19 January 2020). The FFT tells a similar story, indicating a mean exposure time in winter of less than two minutes before uncovered skin would be at high risk of frostbite (Table 2). Values much less than one minute in Figure 2 underscore the dangers of exposing skin for even the briefest of periods on Mount Everest during extreme winter cold events. We note that the monthly mean WCT and FFT shown in Figure 2 are in reasonably good agreement with the National Centers for Environmental Prediction (NCEP) reanalysis-based assessment by Moore and Semple (2011), but we find a less severe cold hazard during the monsoon.

Owing to the high levels of insolation, our COSIPY simulation suggests that the net shortwave radiation flux is the largest energy source for the SCG (Figure 3a). Most of this energy is then dispersed by the net longwave radiation, followed by the turbulent (sensible and latent) heat fluxes, and finally energy for melting. The model results indicate that some meltwater may be generated in the monsoon season, despite the air temperature staying well below 0°C. The majority of the ablation, however, is as sublimation (Figure 3), with cumulative losses of 539mm w.e. in between 23 May 2019 and 30 June 2021: more than nine times the amount of surface melt during the same period (60mm w.e.) (Figure 3b). Temporal variations in sublimation show that although the highest mean rate is in the post-monsoon (October–November), peak rates occur in the winter season, reaching up to 2.5mm w.e. day^{-1}. To put such losses into context, integrating the total sublimation from the colder, windier, and drier months of the post-monsoon and winter (Figure 3d) through the ~150 days of that period indicates that 0.28m w.e. could be ablated during that time. If that figure is also representative of conditions at the summit, and if snow density there is in the region of 300–500kgm^{-3}, then the peak could be expected to 'shrink' by up to 0.5–0.9m during this period (assuming no input of snow via precipitation or wind re-distribution). Given this potential for mass loss, and the considerable efforts expended in measuring the height of Mount Everest (Adhikari and Slater, 2020), we suggest that examining inter-annual variability in the mass balance of the summit could be an interesting direction for future research.

Conclusions

In this short article, we provided the first assessment of wintertime weather meas-

ured by *in situ* stations on Mount Everest. The assessment highlighted the extent of the severe cold hazard on the upper mountain in more detail than has previously been possible, identifying hourly wind chills as low as −83°C and daily means reaching −77°C. This cold hazard amplifies more with the onset of winter than at lower elevations because the lapse rate also steepens in this season. Our investigation also reveals that the combination of strong winds and low relative humidity during the wintertime is enough to drive significant sublimation (2.5mm w.e. day^{-1}) on the upper reaches of Mount Everest. Quantifying mass loss from such previously unexplored seasons and locations is important to understand the impact of climate change on water resources in High Mountain Asia. In the case of Mount Everest, it has additional symbolic value, as it helps illuminate the extent to which the height of Earth's highest mountain is subject to change. Exploring this more could be an interesting avenue for future research.

Conflict of interest statement

The authors declare no conflicts of interest.

References

Adhikari A, **Slater J**. 2020, December 8. Its official: Mount Everest just got a little higher. *The Washington Post*. https://www.washingtonpost.com/world/asia_pacific/mount-everest-height-nepal-china/2020/12/08/a7b3ad1e-389a-11eb-aad9-8959227280c4_story.html.

Bolch T, **Kulkarni A**, **Kääb A** ***et al***. 2012. The state and fate of Himalayan glaciers. *Science* **336**(6079): 310–314.

Heynen M, **Miles E**, **Ragettli S** ***et al***. 2016. Air temperature variability in a high-elevation Himalayan catchment. *Ann. Glaciol.* **57**(71): 212–222.

Hersbach H, **Bell B**, **Berrisford P** ***et al***. 2020. The ERA5 global reanalysis. *Q. J. R. Meteorol. Soc.* **146**(730): 1999–2049.

Hock R, **Bliss A**, **Marzeion BEN** ***et al***. 2019. GlacierMIP – a model intercomparison of global-scale glacier mass-balance models and projections. *J. Glaciol.* **65**(251): 453–467.

Huss M, **Hock R**. 2018. Global-scale hydrological response to future glacier mass loss. *Nat. Clim. Chang.* **8**(2): 135–140.

Immerzeel WW, **Lutz AF**, **Andrade M** ***et al***. 2020. Importance and vulnerability of the world's water towers. *Nature.* **577**(7790): 364–369.

Immerzeel WW, **Petersen L**, **Ragettli S** ***et al***. 2014. The importance of observed gradients of air temperature and precipitation for modeling runoff from a glacierized watershed in the Nepalese Himalayas. *Water Resour. Res.* **50**(3):2212–2226.

Lievens H, **Demuzere M**, **Marshall HP** ***et al***. 2019. Snow depth variability in the Northern Hemisphere mountains observed from space. *Nat. Commun.* **10**(1): 4329.

Litt M, **Shea J**, **Wagnon P** ***et al***. 2019. Glacier ablation and temperature indexed melt models in the Nepalese Himalaya. *Sci. Rep.* **9**(1): 5264.

Matthews T, **Perry LB**, **Koch I** ***et al***. 2020a. Going to extremes: installing the world's highest weather stations on Mount Everest. *Bull. Am. Meteorol. Soc.* **101**(11): E1870–E1890.

Matthews T, **Perry LB**, **Koch I** ***et al***. 2021. Himalayan high: weather stations on Mount Everest reach new heights. *Bull. Am. Meteorol. Soc.* **102**(5): 422–428.

Matthews T, **Perry LB**, **Lane TP** ***et al***. 2020b. Into thick(er) air? Oxygen availability at humans' physiological frontier on Mount Everest. *Iscience* **23**(12): 101718.

Moore GWK, **Semple JL**. 2011. Freezing and frostbite on Mount Everest: new insights into wind chill and freezing times at extreme altitude. *High Alt. Med. Biol.* **12**(3): 271–275.

Nie Y, **Pritchard HD**, **Liu Q** ***et al***. 2021. Glacial change and hydrological implications in the Himalaya and Karakoram. *Nat. Rev. Earth Environ.* **2**(2): 91–106.

Pepin N, **Bradley RS**, **Diaz HF** ***et al***. 2015. Elevation-dependent warming in mountain regions of the world. *Nat. Clim. Chang.* **5**: 424–430.

Potocki M, **Mayewski PA**, **Matthews T** ***et al***. 2022. Mt. Everest's highest glacier is a sentinel for accelerating ice loss. *npj Clim. Atmos. Sci.* **5**(1): 7.

Sauter T, **Schneider C**. 2015. COupled Snowpack and Ice surface energy and MAss balance model. *Geosci. Model Dev.* **47**(3): gmd-8-3911-2015.

Stigter EE, **Litt M**, **Steiner JF** ***et al***. 2018. The importance of snow sublimation on a Himalayan glacier. *Front. Earth Sci.* **6**: 108.

Wagnon P, **Vincent C**, **Arnaud Y** ***et al***. 2013. Seasonal and annual mass balances of Mera and Pokalde glaciers (Nepal Himalaya) since 2007. *Cryosphere* **7**(6): 1769–1786.

Correspondence to: T. C. Sherpa
tenzing.sherpa@icimod.org

© 2023 Royal Meteorological Society.

doi: 10.1002/wea.4374